Mechanical Properties and Flow Characteristics of Dolomite-based Porous Supports for Catalysts Using Different Pore-Forming Agents

Yongjun Li, Heng Wei, Shanjian Liu,* Zhisen He, and Wenjing Zhao

Three kinds of pore-forming agents (corn flour, starch, and biochar) were selected to prepare dolomite-based porous ceramic catalyst carriers with good mechanical properties. Pore-forming agents occupy space within preformed agglomerates, such that after the pyrolysis and sintering have been completed there are spaces within the resulting ceramic material. Porous ceramic samples prepared with biochar exhibited high apparent porosity and water absorption. By contrast, the apparent porosity of the porous ceramic samples prepared with starch as the pore-forming agent was low. When the ratio of the dolomite to quartz sand in the ceramic aggregate was changed from 4:6 to 3:7, the change of the apparent porosity of the porous ceramic samples made with starch as a pore-forming agent was very small, with high bulk density and compressive strength. Compared with corn flour and biochar, starch was less suitable as a pore-forming agent for porous ceramics. The apparent porosity and water absorption of the porous ceramics prepared with biochar as a pore-forming agent decreased slightly. But its bulk density and thermal conductivity were increased. This is mainly attributable to the fact that biochar is lighter, but it performs well in terms of mechanical strength and thermal conductivity.

DOI: 10.15376/biores.17.4.6679-6691

Keywords: Biomass pyrolysis; Porous ceramics; Pore-forming agent; Mechanical properties; Flow characteristics

*Contact information: School of Agricultural Engineering and Food Science, Shandong University of Technology, Zibo, Box 255000, China; *Corresponding author: liushanjian08@163.com*

INTRODUCTION

Biomass pyrolysis technology is an important pathway to achieve the high-value utilization of biomass. However, the bio-oil obtained by conventional pyrolysis has high water content, high acidity, and low content of a single organic component (Jourabchi *et al.* 2016; Montoya *et al.* 2017). Adding catalysts or online catalytic processing of bio-gas during the pyrolysis regulates the content of the resulting bio-oil (Efika *et al.* 2018). A suitable catalyst increases the selectivity of the target compositions, reduces the activation energy during pyrolysis, or lowers the pyrolysis conditions for the formation of target compositions (Zhang *et al.* 2013; Zheng *et al.* 2019).

Biomass pyrolysis catalysts include noble metal catalysts, acid-base catalysts, molecular sieves, and natural ore catalysts (Jiang *et al.* 2013; Li *et al.* 2013). The noble metal catalysts and the molecular sieve catalysts have better directional catalytic effects, but because of their high cost, they are not suitable for large-scale industrial applications. Molecular sieve catalysts prompt the deposition of carbon during pyrolysis because of their

small pore size, which requires frequent regeneration treatments (Kannari *et al.* 2017; Liu *et al.* 2019). Some natural ore catalysts (*e.g.*, calcined dolomite, limestone, olivine) have high catalytic activities, are inexpensive, and are easy to derive, but they do not easily deposit carbon and coke during pyrolysis. Not easy to deposit carbon will lead to high initial activity of the catalyst, catalytic activity decreased rapidly, and shorten the catalyst life (Malik *et al.* 2020). Natural ore catalysts have the disadvantages of low strength and easy fragmentation (Cheah *et al.* 2013). Particles of the catalysts are easily broken into powder when they are in the intense airflow in the reactor, and the catalyst powder is removed from the reactor by the airflow. Thus, the catalytic effects of the natural ore catalysts are weakened (Pourcel *et al.* 2007). In the field of biomass catalytic pyrolysis, efficient precious metal catalysts on cheap natural ore carriers are needed to prepare composite catalysts with suitable activity, high selectivity, and long life.

Porous ceramics have wear resistance, high-temperature resistance, and corrosion resistance. They also have the advantages of the large specific surface area, small bulk density, and high porosity (Sooksaen and Karawatthanaworrakul 2015). Their large pore structure can reduce the direct contact between biochar and catalyst loaded on its internal surface, so it is not easy to block and improve the service life of the catalyst. As a catalyst carrier, porous ceramics are required to have a large specific surface, high mechanical strength, low thermal expansion coefficient, excellent thermal shock resistance, and resistance to acid and alkali corrosion (Wan *et al.* 2020; Zhang *et al.* 2020).

At present, the preparation methods of the porous ceramics are commonly used: pore-forming agent method, foaming method, extrusion molding method, organic foam impregnation method, and particle accumulation method (Alves Xavier *et al.* 2019; Kazantseva and Rashchenko 2016). Generally, different preparation methods and conditions of porous ceramics have a significant effect on their properties.

Zeng *et al.* (2020) used quartz sand and silica powder as porous ceramic aggregates, whereas carboxymethyl cellulose was used as a binder, and corn flour, starch, and bio-char were used as pore-forming agents. Porous ceramic spheres have light weight, large specific surface area, and high mechanical strength. The addition of the quartz sand to the ceramic aggregate was helpful to improve the mechanical strength of the ceramic products (Kouras *et al.* 2017). However, the high melting point of the quartz sand makes the firing process of the porous ceramics very harsh, with high energy consumption. Zinc borate is non-toxic and has good thermal stability. When a certain amount of the zinc borate is added to the ceramic raw materials, the firing temperature can be reduced to about 1000 °C, the firing time is shortened, the expansion coefficient is increased, the firing shrinkage is reduced, and the combination of the ceramic raw materials is firmer (Xi *et al.* 2019). Carboxymethyl cellulose improves the strength of the porous ceramic embryos, increases the mutual bonding between raw materials, and reduces local collapse caused by pore-forming agent exclusion during sintering (Yu *et al.* 2013).

In this study, the parameters of the raw material ratio and pore-forming agent on the microscopic appearance, porosity, water absorption, bulk density, thermal conductivity, and compressive strength of the porous ceramic carrier were analyzed. The fluidization of solid ceramic balls and porous ceramic balls was investigated.

EXPERIMENTAL

Raw Materials

The pore-forming agent method was selected to prepare porous ceramic support capable of supporting a metal ion catalyst. The method is to leave pores in the ceramic body by adding pore-forming agents to the ceramic aggregate and using these pore-forming agents to burn out or volatilize at high temperatures. This process can produce porous products with complex shapes and different pore structures. Dolomite and quartz sand were crushed and ground, selecting 300 to 400 mesh for use. Starch, corn flour, and biochar were used as pore-forming agents. The 120 to 160 mesh fractions were screened on an electronic vibrating screen and placed in an electric blast drying oven for 2 h. Carboxymethylcellulose (CMC) was formulated into a 5% concentration solution by boiling in a water bath for 2 h, then cooled and used.

Processing Flow of Porous Ceramic Ball

The preparation of porous ceramics included batching, forming, drying, sintering, and other processes. First, the ceramic aggregate, pore-forming agent, and fluxing agent were mixed for 30 min. The raw materials were placed in a BY600 vertical ball machine (Weifang Medical Equipment Factory, Weifang, China) for ball processing. During this process, 5% carboxymethylcellulose solution was sprayed to form the globular embryo. The porous ceramic globular embryos were screened to select those meeting the particle size requirements. The others were prepared again after being mashed.

To avoid cracks and deformation of the porous ceramic during the firing process, the prepared ceramic ball and test sample were placed in a cool and ventilated place for 24 h and then processed in a drying oven at 105 °C for 12 h to ensure the moisture content in the ball within 15%.

The determination of the firing curve for the porous ceramics (the heating rate and holding time at each stage) has an impact on the structure and performance of porous ceramics (Allegretta *et al.* 2014). If the temperature change rate is too fast and the firing temperature is too low, the porous ceramics may be prone to crack or to have a black center. Corn flour, starch, and biochar were used as pore-forming agents in the experiment.

According to the characteristics of the porous ceramics aggregate and pore-forming agent, a lower temperature rise rate should be adopted in the temperature range of 250 to 600 °C. In the range of heating to 200 °C, a heating rate of 120 °C/h was used, and in the range of 200 to 600 °C, using a heating rate of 60 °C/h, maintaining at 600 °C for 1 h. Then it entered the sintering stage. The heating rate was 120 and 60 °C/h in the range of 600 to 900 °C and 900 to 1000 °C, respectively. It was maintained at 1000 °C for 2.5 h. Finally, the fired porous ceramic balls and test samples were cooled to room temperature in a muffle furnace and placed into a sealed bag for testing. Each test was done at least three times with a relative error of < 5%. The average values were reported in the results.

Raw Material Ratio and Performance Characterization of Porous Ceramics

The total biomass pyrolysis process is a typical endothermic reaction (Yogalakshmi *et al.* 2022). Compared with biomass particles, porous ceramics can be used as a heat carrier in biomass pyrolysis reactor because of their larger thermal capacity. Through the contact and collision between porous ceramics and biomass powder, the temperature in the pyrolysis reaction area can be relatively uniform, so as to meet the technical requirements of the fast pyrolysis for high temperature rise rate. Porous ceramics serve as catalyst

carriers and heat carriers. Their physical parameters affect the flow and heat, and even affects the composition and content distribution of the thermally cracked products. In addition, the material needs to withstand strong shocks and long-term vibration during the high-temperature biomass pyrolysis gas stream with a severe flowing state. Therefore, the porous ceramic skeleton is required to be resistant to high temperatures, wear, and impact. It also must have a small thermal expansion coefficient.

The effects of the different aggregate ratios and pore-forming agent types on the physical properties (apparent porosity, water absorption, bulk density, thermal conductivity, and compressive strength) of the porous ceramic carriers were investigated, as shown in Table 1. A Quanta250 scanning electron microscope (FEI, Hillsboro, OR, USA) was used to observe the microscopic appearance of the porous ceramic products with different raw material ratios.

Table 1. Mass Ratio of Porous Ceramic Raw Materials (kg)

Serial Number	Type of Pore Forming Agent	Mass of Pore-Forming Agent	Dolomite	Quartz Sand	Zinc Borate	5% CMC
1#	Corn flour	0.8	4	6	1	1
2#	Corn flour	0.8	3	7	1	1
3#	Starch	0.8	4	6	1	1
4#	Starch	0.8	3	7	1	1
5#	Biochar	0.8	4	6	1	1
6#	Biochar	0.8	3	7	1	1

Apparent Porosity, Water Absorption, and Bulk Density of Porous Ceramics

The boiling drainage method (GB/T 1966) was used to determine the apparent porosity, water absorption, and bulk density of the porous ceramics (He *et al.* 2020). First, porous ceramic test samples with no specific requirements on the shape were taken into an ultrasonic cleaning machine. They were placed in a 105 °C drying box for 7 h, drying them to a constant weight. The sample dry weight m_1 was measured using a WCT-1C microcomputer differential thermal balance (Beijing Optical Instrument Factory, Beijing, China). The measured sample was boiled in a beaker with water for 2 h and then cooled to room temperature. The suspended mass m_2 of the saturated sample in water was measured with the electron density meter. The sample was taken out, wiping the water stain on the surface, and the mass m_3 of the saturated sample was measured. The apparent porosity (P_a), water absorption (W), and bulk density (D_b) were calculated using Eqs. 1, 2, and 3, respectively,

$$P_a = \frac{m_3 - m_1}{m_3 - m_2} \times 100\% \quad (1)$$

$$W = \frac{m_3 - m_1}{m_1} \times 100\% \quad (2)$$

$$D_b = \frac{m_1}{m_3 - m_2} \times 100\% \quad (3)$$

where m_1 is the mass of the dry sample (g), m_2 is the apparent mass of the saturated sample (g), and m_3 is the mass of the saturated sample in air (g).

Thermal Conductivity and Compressive Strength of Porous Ceramic Samples

During biomass pyrolysis, porous ceramic is used as a heat carrier to exchange heat with biomass powder. In the fluidized bed and other reactors, the porous ceramic carriers were required to have good mechanical properties and heat transfer performance due to the intense collision contact with the reactor wall and biomass powder.

The prepared porous ceramic was ground into a 25 mm × 10 mm × 5 mm rectangular parallelepiped by using a cutting machine and a grinding machine. The thermal conductivity of the sample at room temperature was tested with a TC3200 series universal thermal conductivity meter (Xi'an Xiaxi Electronic Technology Co., Ltd., Xi'an, China). The porous ceramics were cut into cylinders with a diameter of 20 mm and a height of 20 mm. The compressive strength of the samples was tested with a WDS-5 electronic universal testing machine (Tianshui Hongshan Testing Machine Company, Tianshui, China). The samples for measuring the thermal conductivity and compressive strength of the porous ceramics were the same as the raw materials and sintering processes used for the preparation of the porous ceramic balls, but they differed in appearance. The measured compressive strength was a characteristic value of the mechanical properties for the porous ceramic balls. It did not represent the true value.

Flow Characteristics Test of Porous Ceramics in Fluidized Bed

As the heat carrier and catalyst carrier of the biomass pyrolysis, the flow characteristics of the porous ceramics in the fluidized bed will affect the generation and distribution of the pyrolysis products. The factors affecting the fluidization effect include: fluidization speed, bed height, density, porosity, particle size, and other physical characteristics of the porous ceramics (Wang *et al.* 2021). To study the flow characteristics of the prepared porous ceramic balls in the fluidized bed reactor, a comparative test of the flow characteristics was carried out on a self-made particle fluidization state test-bed. The samples were the prepared porous ceramic balls and a solid ceramic ball (with no added pore-forming agents, corn flour, starch, and biochar) with the same particle size on the market.

The particle fluidization test-bed consisted of a fluidized bed, a pre-distributor, a hood-type air distribution plate, a Roots blower, a glass rotameter, and a U-tube pressure gauge. The bed height and inner diameter of the fluidized bed were 750 and 70 mm, respectively.

The number of the air distribution boards was 19, the aperture was 8 mm, and they were evenly distributed. The air supply of the Roots blower was controlled by a frequency converter. The flow state of the porous ceramic balls and solid ceramic balls with different wind speeds and static bed height was studied, including initial fluidization speed, total bed height, bed pressure, and other parameters.

RESULTS AND DISCUSSION

Effect of Raw Material Ratio on Physical Properties of Porous Ceramics

Micromorphology, apparent porosity, water absorption, and bulk density

The cross-sectional view at 1000 times magnification is shown in Fig. 1. The pore size of the porous ceramic was 5 to 20 μm. The pores were connected, and the specific surface area was large. The pore sizes of the porous ceramic samples (1#, 2#) prepared

using corn flour and starch as pore-forming agents had large differences. There were many large pores. The pore size of the porous ceramic samples was small using biochar as a pore-forming agent. The surface appearance differences of 5# and 6# samples were not obvious.

When the same pore-forming agent was used, the porous ceramic surface became uneven with the increase of the proportion of the dolomite to quartz sand in the aggregate. The number of pores and the specific surface area increased. This was attributed to decomposition of dolomite under high temperature conditions, leaving a large number of pore structures because of the overflow of the gas. However, increasing the proportion of dolomite in ceramic aggregates would reduce the mechanical strength of the porous ceramic products.

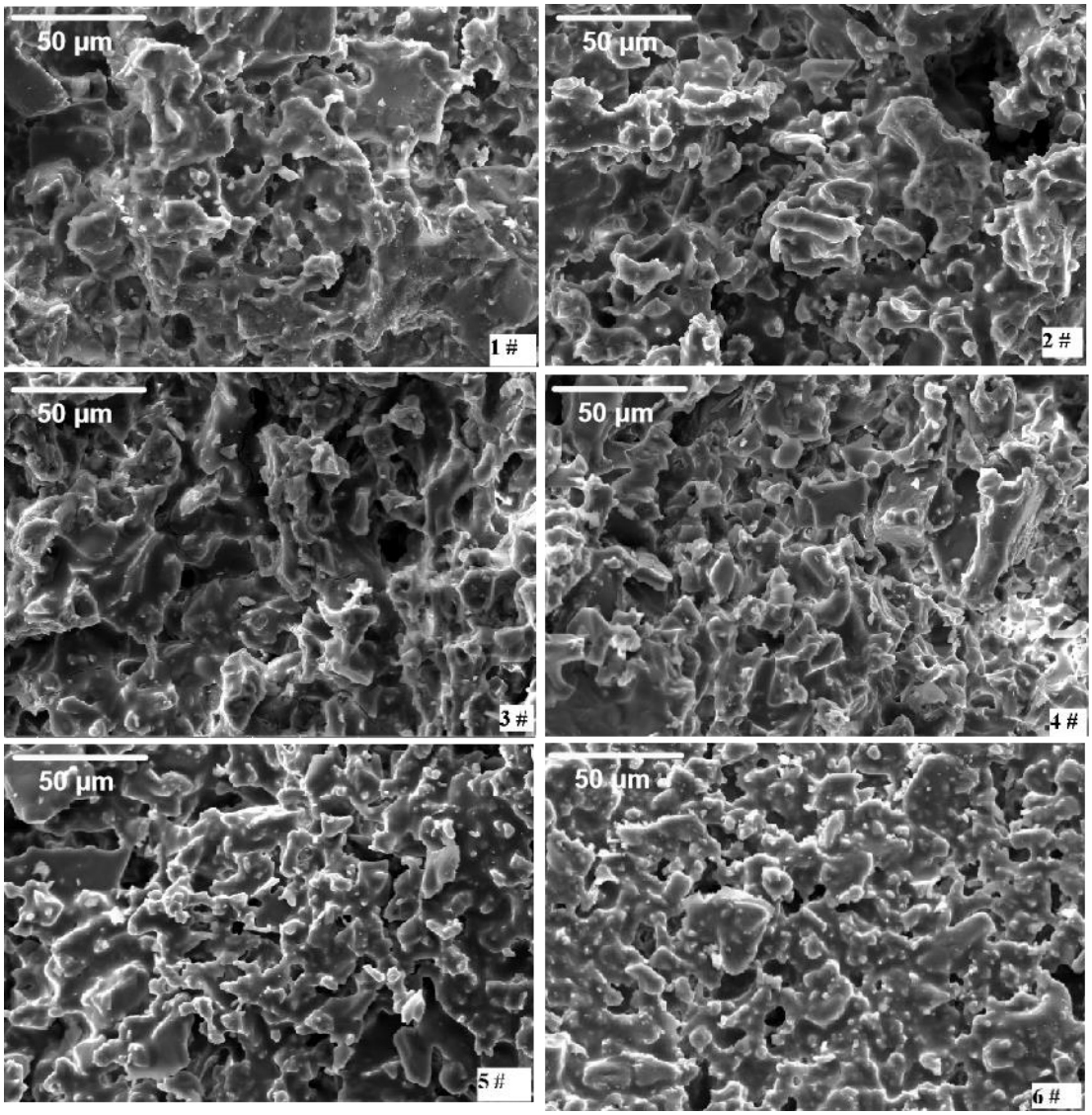

Fig. 1. Scanning electron microscopy of porous ceramics

Figure 2 shows the effects of the different pore-forming agents on apparent porosity, coefficient of the water absorption, and bulk density of the porous ceramics. Compared with corn flour and biochar, the apparent porosity of the porous ceramic samples prepared with starch as pore-forming agent was low. This was attributed to the easy adhesion of the

starch. The pore structure was surrounded by glass phase materials, and the pores were surrounded by large particles (Ishii *et al.* 2020). The bulk density was also increased. The porous ceramics using biochar as pore-forming agent had higher apparent porosity and water absorption. The change of apparent porosity of the porous ceramic samples was inconsistent with the proportion of the dolomite and quartz sand in ceramic aggregate changes from 4:6 to 3:7. When using corn flour as pore-forming agent, the number of the pores and the difference of the pore size were increased with the decrease of the dolomite in aggregate proportion. In some areas, the pore size was 20 μm, resulting in the apparent porosity increase from 38.75% to 44.73%. When starch was used as the pore-forming agent, the apparent porosity of the porous ceramics was almost not affected by the decrease of the dolomite proportion. However, the structure of the porous ceramics was more compact and the pore distribution became more uniform with the increase of the quartz sand proportion. The porosity, apparent porosity and coefficient of the water absorption decreased from 48.0% and 42.1% to 44.8% and 37.5%, respectively using biochar as pore-forming agent. The bulk density increased from 1.14 to 1.20 g·cm^{-3}.

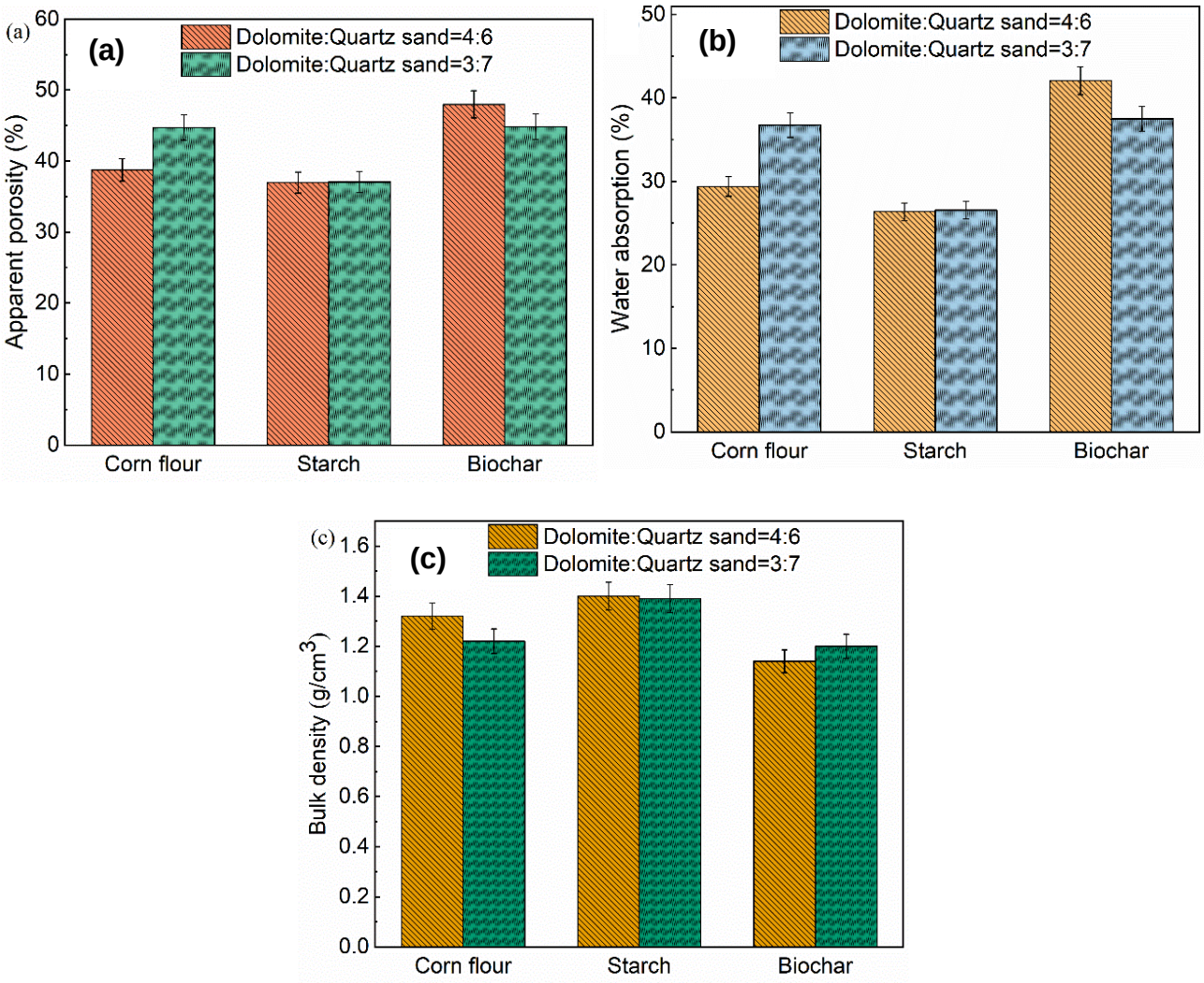

Fig. 2. Effect of different pore formers on a) apparent porosity, b) coefficient of water absorption, and c) bulk density of porous ceramics

Thermal Conductivity and Compressive Strength

Figure 3 shows the effect of corn flour, starch, and biochar as pore-forming agents on thermal conductivity and compressive strength of porous ceramics. When the ratio of the dolomite and quartz sand in ceramic aggregate changed from 4:6 to 3:7, the thermal conductivity of the porous ceramics made with biochar as pore-forming agent increased from 0.436 to 0.639 W/m·K. However, the thermal conductivity of the porous ceramics made with corn powder as pore-forming agent showed little difference. The porous ceramics made with starch as pore-forming agent decreased from 0.652 to 0.557 W/m·K.

Compared with corn flour and biochar, the compressive strength of porous ceramics prepared with starch was almost twice as high as that of porous ceramics prepared with corn flour and biochar. Due to the low apparent porosity and large bulk density, it could be concluded that porous ceramics made with starch as a pore-forming agent had a poor pore-forming effect. Under the experimental conditions, starch was less suitable as a pore-forming agent for porous ceramics. When the ratio of the dolomite to quartz sand in the ceramic aggregate changed from 4:6 to 3:7, the compressive strength of the porous ceramics made with biochar exhibited little difference. This was because the quality of the biochar was light and the density was low. The number of pores formed during the firing process of the porous ceramics was large. Although the proportion of the dolomite in the aggregate was reduced, its compressive strength did not increase significantly. The compressive strength of the porous ceramics prepared with corn flour decreased from 8.41 to 7.42 MPa. This was mainly due to the uneven pore formation during the preparation of the porous ceramics using corn flour.

In summary, thermal conductivity, compressive strength, and apparent porosity are the key consideration indicators using porous ceramics as catalyst and heat carrier during biomass pyrolysis. The porous ceramics made by using corn flour and biochar as pore-forming agents and a 3:7 ratio of dolomite to quartz sand in the ceramic aggregates had better performance.

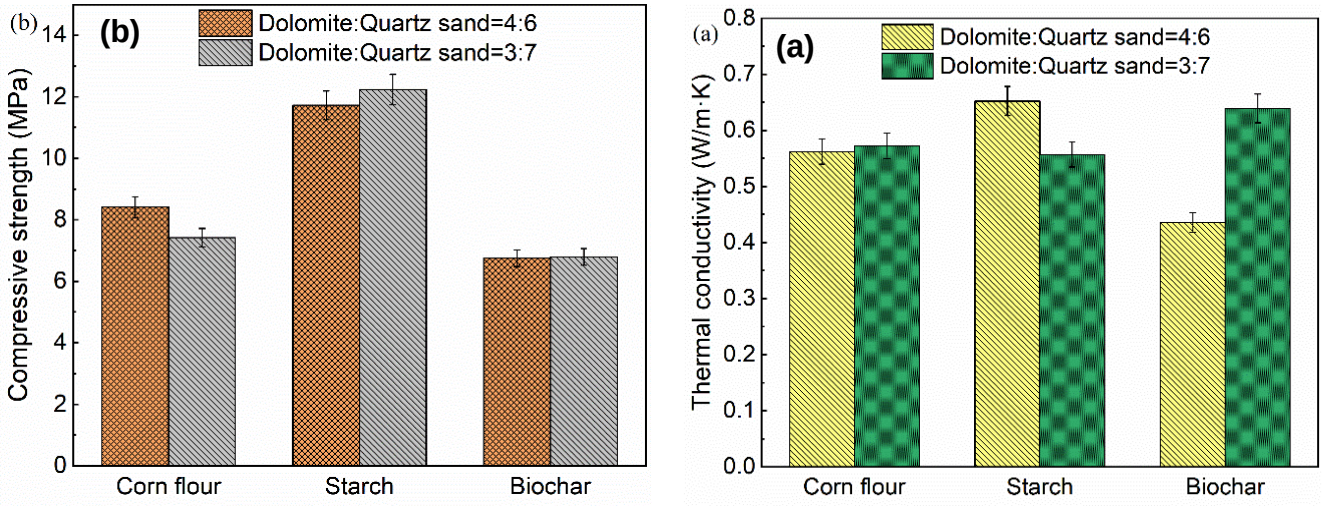

Fig. 3. Effect of different pore-forming agents on a) thermal conductivity and b) compressive strength of porous ceramics

Fluidization Characteristics of Porous Ceramic Balls in Fluidized Bed

The porous ceramic balls were prepared with biochar as pore-forming agent. The ratio of the dolomite to quartz sand was 3:7. The average particle size was 1 to 2 mm, the

apparent porosity was 48.0%, and the bulk density was 1.14 g/cm^{-3}. The fluidization characteristics of commercially available solid ceramic balls were compared. The three static bed heights were 60, 80, and 100 mm.

Relationship Between Static Bed Height and Pressure Drop

The porous ceramic balls and solid ceramic balls were placed in the self-made particle fluidized state test bench according to the heights of the three stationary beds of 60, 80, and 100 mm. The wind speed was increased slowly by adjusting the Roots Fan. The bed pressure during the initial fluidization and full fluidization of the ceramic ball were recorded, as shown in Table 2.

Whether porous or solid ceramic spheres were used, the bed pressure drop at which initial fluidization occurred increased with greater static bed height. When the height of the stationary bed was 60, 80, and 100 mm, the initial fluidization velocity of the porous ceramic balls was 0.859, 0.850, and 0.879 m/s, respectively. The initial fluidization velocities of the solid ceramic balls were 0.790, 0.794, and 0.821 m/s, respectively. The initial fluidization velocity showed little difference with changes in the static bed height. The bed pressure drop increased with the increase of the fluidization speed. There was a linear relationship between them. When the bed material was fully fluidized (the fluidization wind speed reached a certain value), the bed pressure drop reached the maximum value. Even if the fluidization wind speed increased, the bed pressure drop no longer changed with a stable value. Compared with the solid ceramic balls, the initial fluidizing pressure drop and the final pressure drop were only 0.35 to 0.43 of the former at different static bed heights using the porous ceramic balls as the fluidizing medium. This result indicated that the porous ceramic balls were easily fluidized at the same particle size.

Table 2. Relationship between Static Bed Height and Bed Pressure Drop

Static Bed Height (mm)	Initial Fluidization Pressure Drop (Pa)		Final Pressure Drop (Pa)	
	Porous ceramic ball	Solid ceramic ball	Porous ceramic ball	Solid ceramic ball
60	200	500	210	600
80	330	850	400	930
100	500	1250	520	1300

Relationship between Fluidization Wind Speed and Bed Height

Figure 4 shows the changes in the total height of the dilute phase zone, dense phase zone, and bed of fluidized bed with increasing fluidized gas velocity when the static bed height of the porous ceramic balls and solid ceramic balls were both 80 mm. When the particle size and the height of the stationary bed were the same, the bed height did not change when the initial fluidization speed was reached. With the increase of the fluidized gas velocity, the bed height of the porous ceramic balls and solid ceramic balls increased approximately linearly. However, the total bed height increased slowly and flattened with the fluidized wind speed reaching a certain value. The relationship between bed height of the porous ceramic ball and fluidization velocity was as follows:

$$y = 17.13x + 10.79 \quad (4)$$

The regression relationship between bed height and fluidization velocity was as follows:

$$y = 10.83x + 5.29 \quad (5)$$

where y is bed height, x is fluidization velocity.

At the same fluidizing wind speed, the fluidization effect of the porous ceramic balls was better than that of solid ceramic balls. The main reason is that the porosity of the porous ceramic spheres was high and the bulk density was small. The lower density spheres were easier to fluidize under the action of the same wind. At the beginning of the fluidization, the bed was almost completely dense. As the fluidization speed increased, a dense phase region with a smaller particle density began to appear. The total bed height, the bed height in the dense phase zone, and the bed height in the rare phase zone all increased with the fluidization wind speed continuously increasing. When the fluidized wind speed reached a certain value, the height of the bed in the dilute phase zone was equal to the height of the bed in the dense phase zone. If the fluidized wind speed increased continuously, the height of the bed in the rare phase zone would exceed the height of the bed in the dense phase zone. In the whole process, the rate of increase of the bed height in the dilute phase zone was greater than that in the dense phase zone.

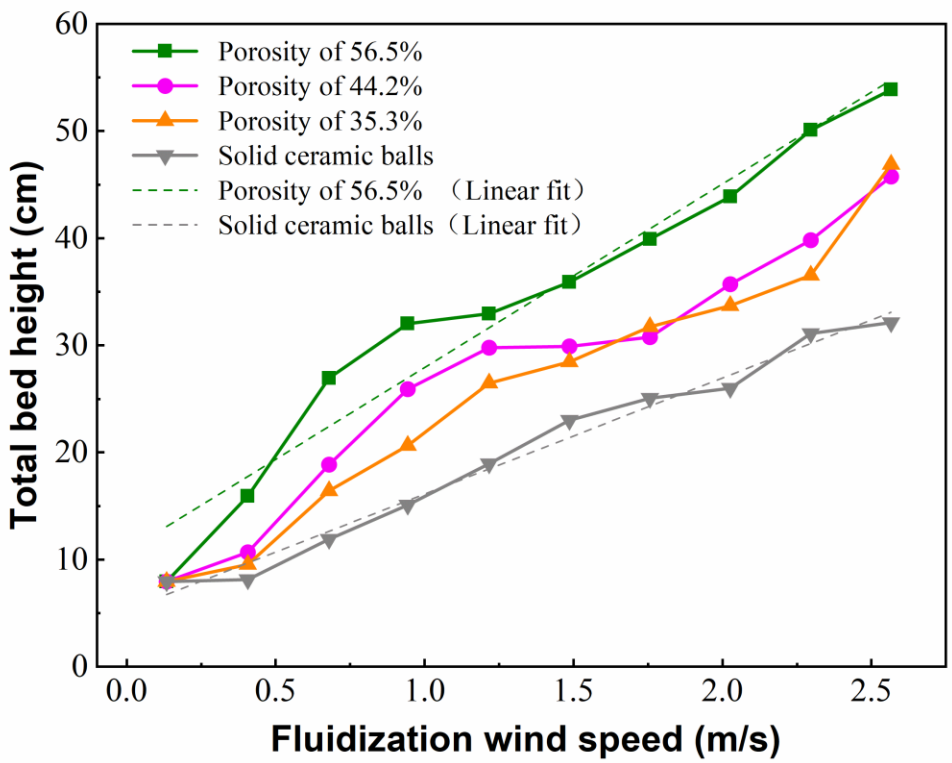

Fig. 4. Fluidization wind speed and bed height of porous ceramic balls and solid ceramic balls

CONCLUSIONS

1. When the ratio of the dolomite to quartz sand in the ceramic aggregate was changed from 4:6 to 3:7, the apparent porosity of the prepared porous ceramic samples using starch as the pore-forming agent changed little. When biochar was used as a pore-forming agent, the pores formed by the prepared porous ceramic samples were reduced.
2. The effect on the thermal conductivity of the porous ceramics made with corn flour as a pore-forming agent was small. However, the thermal conductivity of the porous

ceramics prepared with starch as a pore-forming agent decreased from 0.652 to 0.557 W/m·K. Compared with corn flour and biochar, starch was less suitable as a pore-forming agent for porous ceramics.

3. Compared with solid ceramic balls, the initial fluidization pressure drop and final pressure drop of the porous ceramic balls were only 0.35 to 0.43 of the former at different static bed heights. The bed height increased significantly.

ACKNOWLEDGEMENTS

The research was sponsored by the National Key Research and Development Program of China (No. 2019YFD1100602), National Natural Science Foundation of China (No. 52176193), Shandong Provincial Natural Science Foundation, China (No. ZR2020ME184), and SDUT & Zhangdian City Integration Development Project (No.2021JSCG0013).

REFERENCES CITED

Allegretta, I., Eramo, G., Pinto, D., and Hein, A. (2014). "The effect of temper on the thermal conductivity of traditional ceramics: Nature, percentage and granulometry," *Thermochimica Acta* 581, 100-109. DOI: 10.1016/j.tca.2014.02.024

Alves Xavier, L., de Oliveira, T. V., Klitzke, W., Mariano, A. B., Eiras, D., and Vieira, R. B. (2019). "Influence of thermally modified clays and inexpensive pore-generating and strength improving agents on the properties of porous ceramic membrane," *Applied Clay Science* 168, 260-268. DOI: 10.1016/j.clay.2018.11.025

Cheah, S., Gaston, K. R., Parent, Y. O., Jarvis, M. W., Vinzant, T. B., Smith, K. M., Thornburg, N. E., Nimlos, M. R., and Magrini-Bair, K. A. (2013). "Nickel cerium olivine catalyst for catalytic gasification of biomass," *Applied Catalysis B: Environmental* 134-135, 34-45. DOI: 10.1016/j.apcatb.2012.12.022

Efika, C. E., Onwudili, J. A., and Williams, P. T. (2018). "Influence of heating rates on the products of high-temperature pyrolysis of waste wood pellets and biomass model compounds," *Waste Management* 76, 497-506. DOI: 10.1016/j.wasman.2018.03.021

He, S., Zhou, P., Ma, Z., Deng, W., Zhang, H., Chi, Z., Liu, W., and Liu, Z. (2020). "Experimental study on transient performance of the loop heat pipe with a pouring porous wick," *Applied Thermal Engineering* 164, article no. 114450. DOI: 10.1016/j.applthermaleng.2019.114450

Ishii, K., Shimizu, M., Sameshima, H., Samitsu, S., Ishigaki, T., and Uchikoshi, T. (2020). "Fabrication of porous (Ba,Sr)(Co,Fe)O_3-δ (BSCF) ceramics using gelatinization and retrogradation phenomena of starch as pore-forming agent," *Ceramics International* 46 (9), 13047-13053. DOI: 10.1016/j.ceramint.2020.02.075

Jiang, T., Wang, W., and Han, B. (2013). "Catalytic hydroxylation of benzene to phenol with hydrogen peroxide using catalysts based on molecular sieves," *New Journal of Chemistry* 37(6). DOI: 10.1039/c3nj41163j

Jourabchi, S. A., Ng, H. K., Gan, S., and Yap, Z. Y. (2016). "Investigation on the quality of bio-oil produced through fast pyrolysis of biomass-polymer waste mixture," *IOP Conference Series: Earth and Environmental Science* 36. DOI: 10.1088/1755-

1315/36/1/012044

Kannari, N., Oyama, Y., and Takarada, T. (2017). "Catalytic decomposition of tar derived from biomass pyrolysis using Ni-loaded chicken dropping catalysts," *International Journal of Hydrogen Energy* 42(15), 9611-9618. DOI: 10.1016/j.ijhydene.2017.02.168

Kazantseva, L. K., and Rashchenko, S. V. (2016). "Optimization of porous heat-insulating ceramics manufacturing from zeolitic rocks," *Ceramics International* 42 (16), 19250-19256. DOI: 10.1016/j.ceramint.2016.09.091

Kouras, N., Harabi, A., Bouzerara, F., Foughali, L., Policicchio, A., Stelitano, S., Galiano, F., and Figoli, A. (2017). "Macro-porous ceramic supports for membranes prepared from quartz sand and calcite mixtures," *Journal of the European Ceramic Society* 37 (9), 3159-3165. DOI: 10.1016/j.jeurceramsoc.2017.03.059

Li, L., Quan, K., Xu, J., Liu, F., Liu, S., Yu, S., Xie, C., Zhang, B., and Ge, X. (2013). "Mesoporous molecular sieves K_2O/Ba(Ca or Mg)-MCM-41 with base sites as heterogeneous catalysts for the production of liquid hydrocarbon fuel from catalytic cracking of rubber seed oil," *Green Chemistry* 15(9). DOI: 10.1039/c3gc40796a

Liu, Y., Yu, H., Liu, J., and Chen, D. (2019). "Catalytic characteristics of innovative Ni/slag catalysts for syngas production and tar removal from biomass pyrolysis," *International Journal of Hydrogen Energy* 44(23), 11848-11860. DOI: 10.1016/j.ijhydene.2019.03.024

Malik, N., Bulasara, V.K., and Basu, S. (2020). "Preparation of novel porous ceramic microfiltration membranes from fly ash, kaolin and dolomite mixtures," *Ceramics International* 46 (5), 6889-6898. DOI: 10.1016/j.ceramint.2019.11.184

Montoya, J., Pecha, B., Roman, D., Janna, F. C., and Garcia-Perez, M. (2017). "Effect of temperature and heating rate on product distribution from the pyrolysis of sugarcane bagasse in a hot plate reactor," *Journal of Analytical and Applied Pyrolysis* 123, 347-363. DOI: 10.1016/j.jaap.2016.11.008

Pourcel, F., Jomaa, W., Puiggali, J. R., and Rouleau, L. (2007). "Criterion for crack initiation during drying: Alumina porous ceramic strength improvement," *Powder Technology* 172(2), 120-127. DOI: 10.1016/j.powtec.2006.10.041

Sooksaen, P., and Karawatthanaworrakul, S. (2015). "The properties of Southern Thailand clay-based porous ceramics fabricated from different pore size templates," *Applied Clay Science* 104, 295-302. DOI: 10.1016/j.clay.2014.12.009

Wan, L., Guo, X., Li, K., and Yan, J. (2020). "Preparation of porous SiC-Al_2O_3 ceramics with spherical shell structures of large surface area and high strength," *Ceramics International* 46 (8, Part A), 10325-10331. DOI: 10.1016/j.ceramint.2020.01.028

Wang, R., Hou, A., and Wu, Z. (2021). "Tomography-based investigation of flow and heat transfer inside reticulated porous ceramics," *Applied Thermal Engineering* 184, article no. 116115. DOI: 10.1016/j.applthermaleng.2020.116115

Xi, J., Lu, B., Chen, J., Chen, G., Shang, F., Xu, J., Zhou, C., and Yuan, C. (2019). "Ultralow sintering temperature and permittivity with excellent thermal stability in novel borate glass-ceramics," *Journal of Non-Crystalline Solids* 521, article no. 119527. DOI: 10.1016/j.jnoncrysol.2019.119527

Yogalakshmi, K. N., Poornima, D. T., Sivashanmugam, P., Kavitha, S., Kannah R., Y., Varjani, S., AdishKumar, S., Kumar, G., and Banu J., R. (2022). "Lignocellulosic biomass-based pyrolysis: A comprehensive review," *Chemosphere* 286, article no. 131824. DOI: 10.1016/j.chemosphere.2021.131824

Yu, J., Yang, J., Zeng, Q., and Huang, Y. (2013). "Effect of carboxymethyl cellulose

addition on the properties of Si_3N_4 ceramic foams," *Ceramics International* 39(3), 2775-2779. DOI: 10.1016/j.ceramint.2012.09.044

Zeng, L., Sun, H., Peng, T., and Zheng, W. (2020). "Preparation of porous glass-ceramics from coal fly ash and asbestos tailings by high-temperature pore-forming," *Waste Management* 106, 184-192. DOI: 10.1016/j.wasman.2020.03.008

Zhang, Y., Li, W., Zhang, S., Xu, Q., and Yan, Y. (2013). "Hydrogen production by the catalytic reforming of volatile from biomass pyrolysis over a bimetallic catalyst," *Energy Sources, Part A: Recovery, Utilization, and Environmental Effects* 35(21), 1975-1982. DOI: 10.1080/15567036.2011.580327

Zhang, Y., Wu, Y., Yang, X., Li, D., Zhang, X., Dong, X., Yao, X., Liu, J., and Guo, A. (2020). "High-strength thermal insulating mullite nanofibrous porous ceramics," *Journal of the European Ceramic Society* 40(5), 2090-2096. DOI: 10.1016/j.jeurceramsoc.2020.01.011

Zheng, Y., Tao, L., Huang, Y., Liu, C., Wang, Z., and Zheng, Z. (2019). "Improving aromatic hydrocarbon content from catalytic pyrolysis upgrading of biomass on a CaO/HZSM-5 dual-catalyst," *Journal of Analytical and Applied Pyrolysis* 140, 355-366. DOI: 10.1016/j.jaap.2019.04.014

Article submitted: June 19, 2022; Peer review completed: August 27, 2022; Revised version received and accepted: September 6, 2022; Published: October 14, 2022.
DOI: 10.15376/biores.17.4.6679-6691